Hindawi
Advances in Condensed Matter Physics
Volume 2017, Article ID 4396015, 8 pages
https://doi.org/10.1155/2017/4396015

Research Article

Stability of Bar Code Information Stored in Magnetic Nanowire Arrays

Eduardo Cisternas,[1] Eugenio E. Vogel,[1,2] and Julián Faúndez[1]

[1]*Departamento de Ciencias Físicas, Universidad de La Frontera, Casilla 54-D, Temuco, Chile*
[2]*Center for the Development of Nanoscience and Nanotechnology (CEDENNA), 9170124 Santiago, Chile*

Correspondence should be addressed to Eugenio E. Vogel; eugenio.vogel@ufrontera.cl

Received 18 December 2016; Accepted 2 April 2017; Published 19 April 2017

Academic Editor: Mohindar S. Seehra

Firmware applications such as security codes, magnetic keys, and similar products can be stored in magnetic bar codes similar to optical bar codes. This can be achieved on the triangular lattice present in porous alumina, whose pori can be filled by magnetic material, over which magnetic bar codes can be inscribed. We study the conditions to improve the durability of the stored information by minimizing the repulsive energy among wires with parallel magnetization within the same bar but interacting with attractive energy with wires in the neighboring bar. The following parameters are varied to minimize the energy of the system: relative amount of magnetization orientation within the bar code area in any orientation, width of the bars, and distribution of wider bars to the outside or to the inside of the code. It is found that durability of the code is favored for equal amount of magnetization in each direction, abundance of narrow bars trying to locate a few wider ones towards the center. Three real commercial optical bar codes taken at random were mapped into magnetic bar codes; it is found that the corresponding magnetic energies are similar to those analyzed here which provides a realistic test for this approach.

1. Introduction

Optical bar codes are frequently used to store coded information for multiple purposes. However, this technology has at least two disadvantages for some specific uses: they are visible to anybody so they could be replicated (a single photocopy is enough) and they can get easily damaged by peeling or scratching. We propose here to store the same information in the form of magnetic bar codes stored by arrays of magnetic nanowires trapped in the porous membrane used to produce them [1–6]. Such information is now hidden (not easily replicated) and friction on them would not hamper the information.

The idea is the same as the one proposed to store symbols (letters for example) [7, 8] in these systems. There is one hazard present: magnetization reversal [3, 9–11] can affect the stored information. To improve the duration of the stored information two mechanisms have been recently proposed: the inscription of an opposite ferromagnetic band (OFB) and the storage of the symbol in a set of bisegmented magnetic nanowires [12, 13]. Although the second technique yields the best results in terms of canceling completely repulsive energies coming from magnetic segments interactions it is probably expensive at the moment of fabrication. On the other hand, the first technique is easier to implement on any array of magnetic nanowires by means of a powerful magnetic tip orienting the magnetization of the selected wires in the desired direction [7]. The same procedure can be used to inscribe magnetic bars.

For the present proposal OFB is not necessary since the ferromagnetic sectors alternate with opposite orientations within the code thus providing a built-in stabilization mechanism similar to the OFB for the case of symbols. In Figure 1 we provide a scheme which serves to define the system, its main parameters, and the way a magnetic bar code can be realized. We are not aware of any experiment resembling code bars like those presented in Figure 1 and the others to follow below. However, it does not seem to be a problem to produce such orientations after the work by Jaafar et al. [7] where they present a figure spelling CSIC (Consejo Superior

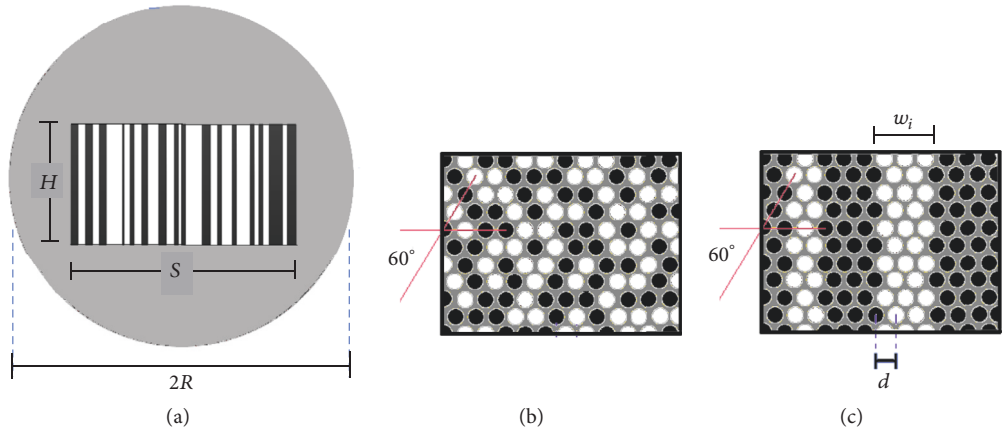

Figure 1: (a) Top view of the schematic representation of the inscription of information on magnetic bar codes inside a circular membrane of radius R and height $2L$. Wires are perpendicular to the page penetrating it for the full length $2L$. Black areas represent wire magnetizations pointing up; white areas represent wire magnetization pointing down; gray areas indicate random orientation. An arbitrary bar code is shown in a rectangle of length S and height H. (b) Magnification of a possible background area presenting no magnetic order with total nil magnetization; (c) magnification of the bar code area showing ideal magnetization profiles producing bars with generic width w_i, where i runs over all bars.

de Investigaciones Cientificas). In our proposal orienting rectangular sectors (like the bar codes proposed here) should be simpler than inscribing curved symbols. Other properties of the system under study will be fully described in next section where the system and the methodology will be explained. Then in Section 3 we present the main results and in Section 4 we present the main conclusions.

2. System and Methodology

2.1. System. Figure 1 illustrates in a general way the main characteristics of the systems studied here. The starting point is a circular alumina membrane whose pori are filled in with magnetic material (i.e., cobalt) in order to produce wires or rods. We assume here ideal conditions. All wires are alike and perfectly cylindrical; they have the same length $2L$ (perpendicular to the illustration in Figure 1) equivalent to the height of the membrane, whose radius is R. The radius of each cylinder is b. The axes of any pair of interacting cylinders are separated by a distance $d \leq D \leq 2R$ distributed over a triangular lattice of lattice constant d. In real wires these conditions could not be entirely satisfied (i.e., cross section is not always circular and radius is not completely constant along the tube). However, these are minor modifications to the geometry which still can be described in the ideal terms just given. Thus, results can be affected by some noise but still following the trends discussed below. In practical terms we consider here the following dimensions for the wires: $2L = 12000$ nm, $d = 700$ nm, and $b = 260$ nm which are realistic geometrical characteristics taken from the literature [1, 2, 5, 14]. In addition we assume a dominant shape anisotropy so the magnetization is along the cylindrical axis in any of the two directions.

Within this bundle of magnetic nanowires we define a rectangular area of $S = 70000$ nm (100 wires) along the longer ("horizontal") dimension and $H = 27886$ nm (46 wires) along the shorter ("vertical") dimension as depicted in Figure 1. The number of wires within the rectangular area is $n = 4600$. The radius of the membrane is $R = 45500$ nm. Outside the rectangle the orientation of the individual magnetization of each wire is at random producing a nil result for the total magnetization [7, 15]. Inside the rectangle different codes will be inscribed by means of bars of height H and width w_i alternating the orientation of the individual magnetization and regulating the widths w_i to produce a desired code. The general geometrical characteristics of this system are kept fixed in all calculations below. We will vary the net magnetization of the code, the number of bars q, the width of the bars ($w_i = S/q$ for bars of equal width), and the distributions of wide and narrow bands along the horizontal direction.

Calculations below can be done for any kind of magnetic material and this will be reflected in the saturation magnetization which will be formally introduced below; other properties follow from the geometrical setup. In the present calculation we use data for Co due to the high coercivity reached by this material which reaches coercivity values of 1000 to 1500 Oe and saturation magnetization of about 1.26×10^6 A/m [16]. Co can grow in two different forms and we assume here that most of the wires grow in such a way that the shape anisotropy (magnetization along the axis) will prevail. However, in real systems some portions of the rod could be in fact multidomains with different magnetization orientations. In such cases, the wire will contribute with less repulsive energy than the one calculated below. Nevertheless, this would be a less critical condition for reversal which is what we are trying to avoid. In other words, our calculations below are valid under the less favorable conditions, which is the case of full monodomains within each wire forming the bar.

2.2. Methodology. The magnetostatic interaction between two parallel cylinders has been expressed in an integral form involving Bessel functions [17] in an approach that

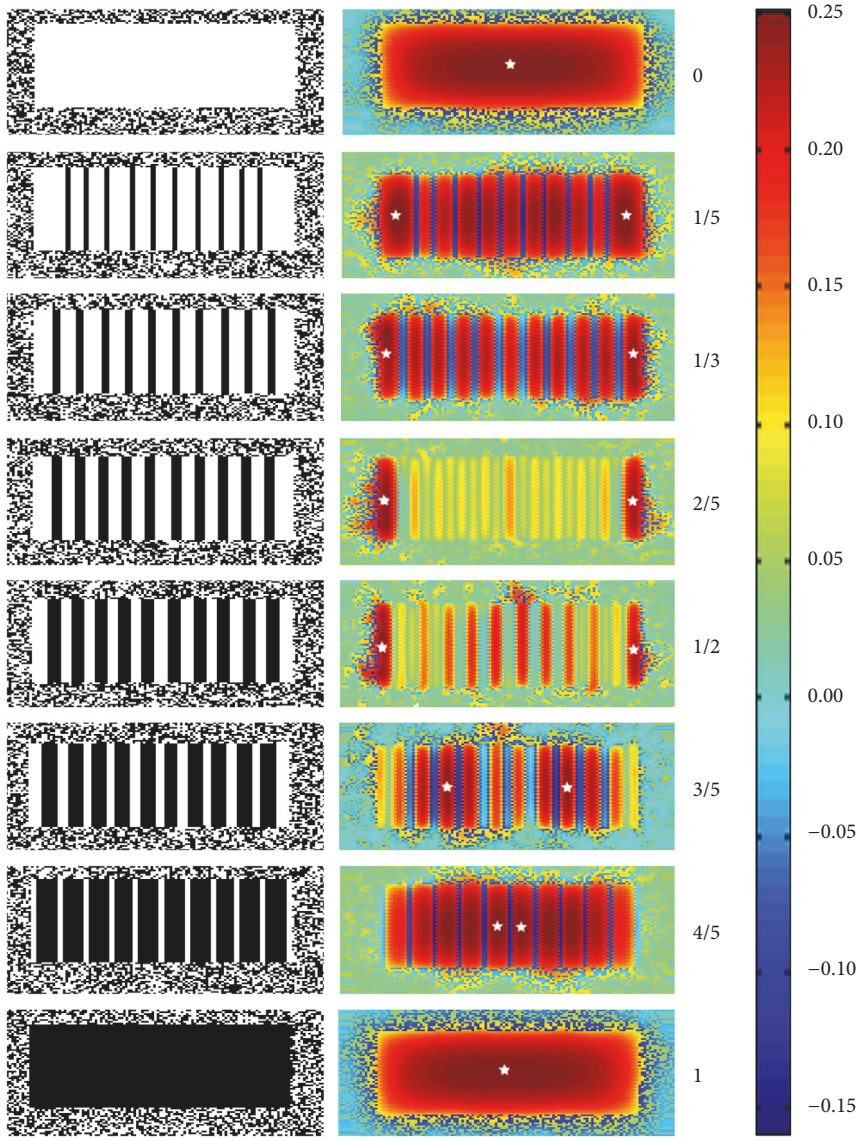

FIGURE 2: Progressive increase of the fraction of area x with up magnetization. The starting point is the rectangle with $x = 0.0$, namely, the magnetization of all wires in the rectangle pointing down. The left-hand column illustrates the magnetization imposed scheme while the right-hand column gives the energy map with reddish colors marking higher repulsive energy sectors: a palette code is given to the far right. Stars indicate the positions of the wire with the highest repulsive energy.

follows a more general study on the interaction between two magnetic objects [18]. Under the condition $b \ll 2L$, the magnetostatic energy between any two parallel wires separated by a distance D having uniform axial magnetization can put in terms of a general algebraic expression beyond the dipole approximation [12, 19]. For the case under study such expression reduces to

$$\widetilde{E}^{\mathrm{pair}(i,j)} = \sigma_i \sigma_j \frac{b^2}{8LD}\left[\eta_0 + \eta_2\left(\frac{b}{D}\right)^2 + 5\eta_4\left(\frac{b}{D}\right)^4\right], \quad (1)$$

where σ_i takes the value ± 1 to reflect the magnetization polarization with respect to the axis of the cylinder, while the functions η_i are given by simple algebraic expressions in terms of L and D:

$$\eta_0 = 2\left[1 - \frac{D}{\sqrt{D^2 + 4L^2}}\right],$$
$$\eta_2 = \frac{1}{2}\left[1 - \frac{D^3\left(D^2 - 8L^2\right)}{\left(D^2 + 4L^2\right)^{5/2}}\right], \quad (2)$$
$$\eta_4 = \frac{3}{32}\left[1 - \frac{D^5\left(3D^4 - 96L^2D^2 + 128L^4\right)}{3\left(D^2 + 4L^2\right)^{9/2}}\right].$$

Expression (1) yields the magnetostatic energy in units of $\mu_0 M_0^2 V$, where μ_0 is the magnetic permeability of vacuum,

while M_0 and $V = 2Lb^2\pi$ are the saturation magnetization and the volume of each cylinder, respectively (M_0 value was already quoted above). All energies in this work are expressed in terms of this unit. This approach allows fast evaluation of different configurations with high enough accuracy, avoiding lengthy computer calculations based on integrals of expressions involving Bessel functions [17] which lead to results harder to interpret and analyze.

Thus, to obtain the total energy of a magnetization configuration we must add all the $N(N-1)/2$ contributions for a membrane containing N wires:

$$E_{\text{tot}} = \sum_{i<j} \tilde{E}^{\text{pair}(i,j)}. \tag{3}$$

The average interaction energy per wire is simply given by

$$E_{\text{average}} = \frac{E_{\text{tot}}}{n}, \tag{4}$$

where n is the total number of wires within the rectangular zone.

On the other hand we can calculate the energy contribution of any wire (the ith wire for instance) by adding the interactions with all the other wires in the membrane

$$E_i = \sum_{j\neq i} \tilde{E}^{\text{pair}(i,j)}. \tag{5}$$

In particular this calculation allows us to single out the wire which is mostly repelled by the set of all the others which makes it a candidate to trigger the magnetization reversal we would like to avoid. This particular energy will be called E_{max} from now on.

We will add all interactions within the bar code in different configurations looking for the most stable conditions (lower repulsive energy) to store the bar code information.

3. Results and Discussions

We will first investigate the variations of repulsive energy in the system as we change the area of one relative orientation of the magnetization with respect to the other. So we prepare the rectangle with all wires magnetized in one direction (down say) as shown by the white rectangle of the upper part of Figure 2. Then, we introduce bars with magnetization pointing in the opposite direction shown in black, thus varying the relative area of up magnetization with respect to the total area of the rectangle previously defined in Figure 1. Let us call x the fraction of the area with up magnetization contained in the black bars depicted in Figure 2. Then, we increase x in the progression 0.0, 1/5, 1/3, 2/5, 1/2, 3/5, 4/5, and 1.0. The left-hand side of Figure 2 shows the relative magnetization orientation while the right-hand side gives the repulsive energy in color code: reddish means areas of higher magnetostatic repulsive energy (a palette is also given to the right of this figure); white stars indicate the points of maximum repulsive energy E_{max}.

The corresponding values for previous maximum energies are given in the top part of Figure 3 by means of stars. The lower part of this same figure uses bullets to report the average energy for the corresponding bar code. As it can be noticed these results are nonsymmetric with respect to $x = 0.5$ since the original bar distribution is not. This can be realized upon comparing the bar distributions for cases of coverage $x = 1/5$ and $x = 4/5$ leading to different positions for the points of highest repulsive energy (white stars) in Figure 2; a similar analysis can be done upon comparing concentrations $x = 2/5$ and $x = 3/5$.

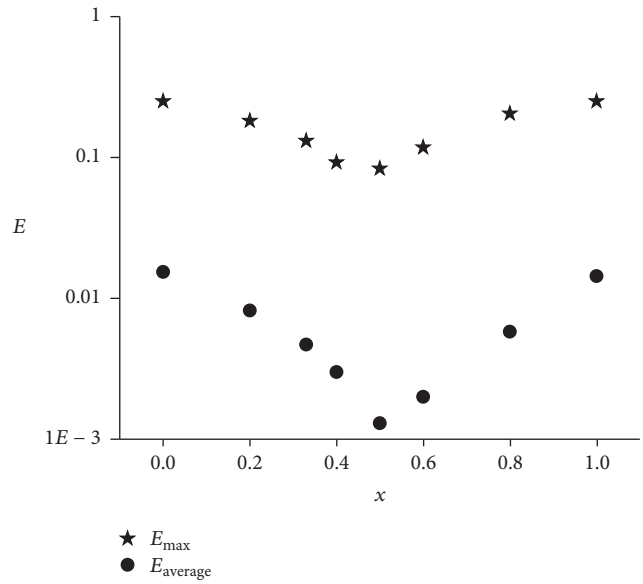

Figure 3: Bottom: average repulsive energy per wire in the bar code as function of the presence of up magnetization; top: maximum repulsive energy for any wire in the configuration with the corresponding proportion of up magnetization (wire located at the white star position in the previous figure).

It follows from previous figure that the repulsion is minimized for equal areas magnetically oriented in opposite senses ($x \approx 0.5$). We fix x at 0.5 and investigate the influence of the width of the bars. The scheme is shown in Figure 4 where the left-hand side shows the magnetic configuration of the bars within the rectangle for bars of equal widths $w_i = S/q$, where q (the total number of bars) takes the values 2, 4, 6, 8, 10, 12, and 16. The right-hand side of this figure gives the repulsive energy map: reddish means higher magnetic repulsion (a palette is also given to the right of this figure). Stars indicate the points of maximum repulsive energy whose values are reported in the upper part of Figure 5 as a function of q. The lower part of this figure gives the average repulsive energy as a function of q. The latter tends to decrease with the narrowing of the bars, but this tendency is nonmonotonic. This is a mere manifestation of the small size of our system: we need to divide the 100 wires into two sections of 50 and then into 4 sections of 4, so far so good. However, commensuration effects arise when trying to divide the 100 wires into 6 or 8 sectors. Then some additional repulsive energy is injected due to the lack of compensation of magnetization for consecutive sectors. Since this is not along the line of the main results sought for here we just mention this curiosity and continue to the general discussion.

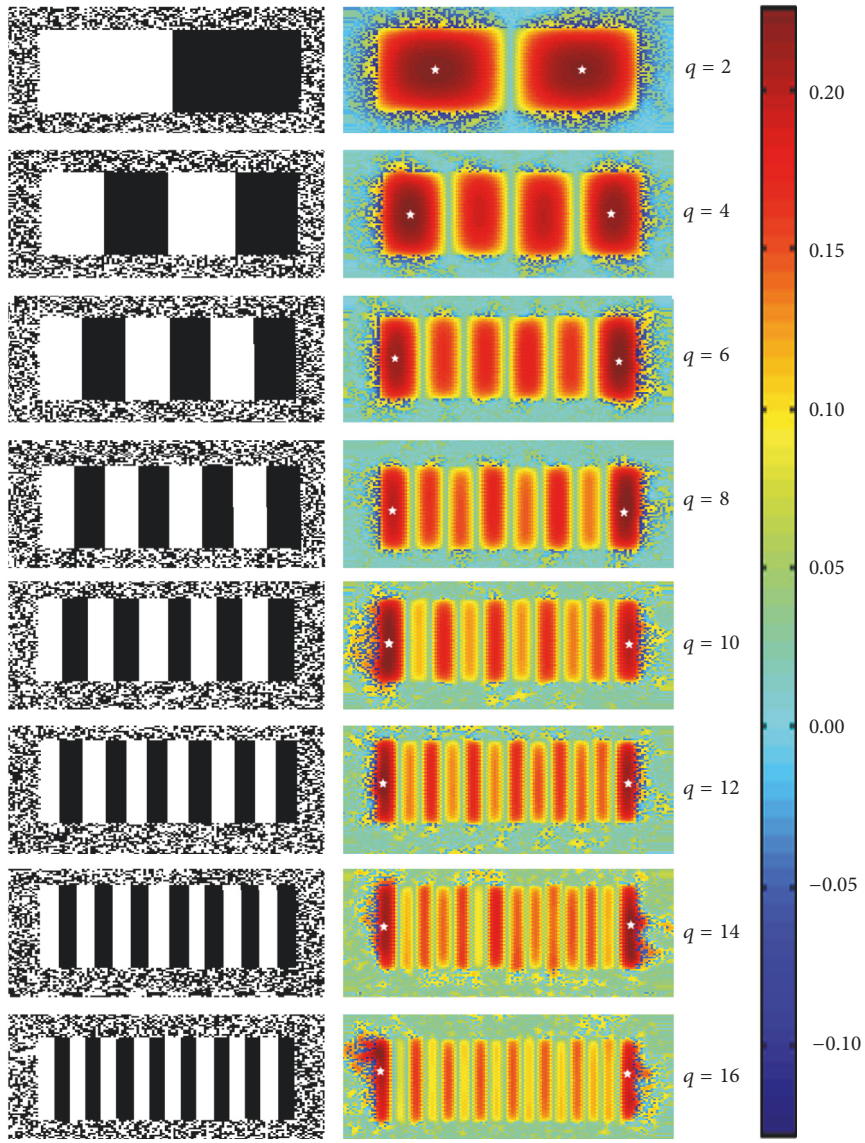

FIGURE 4: Configurations with increasing number q of equal bars (narrowing the width $w_i \approx S/q$ for all bars). To the left the magnetic sectors are defined schematically. To the right the actual energy map is presented with reddish colors for the most repulsive areas: a palette code is given to the far right. White stars identify the points with maximum repulsive energy.

Previous result indicates that narrow bars should be preferred, but there is a tendency to saturate. So actually it is more accurate to say that wide bars should be avoided. Nevertheless different widths are necessary in any bar code. Where should wide bars go in order to better stabilize the stored information? This issue is addressed in Figure 6 where two wide bars alternate positions with 4 narrower bars. The corresponding maximum energy for each configuration is given on top of each one. Wider bars minimize energy in the central positions. It follows that when defining the width of the codes narrower bars should be placed towards the outside positions leaving the wider bars towards the center of the code.

Finally we considered codes taken from real optical bar codes found in three commercial products picked at random. Part of each code is mapped into the rectangular area $S \times H$ as shown in Figure 7. The corresponding maximum energy is given to the right of the corresponding magnetic bar code. The top one, with unbalanced magnetization favoring white areas and with wide bars all over the code, presents the higher maximum magnetostatic energy. The other two codes with similar white and black areas and with narrower bands present lower energies as expected. The three energies are in the ranges covered by Figures 3 and 5 and the two distributions given in Figure 6.

Previous minimization energy features are independent so they can be properly combined to actually minimize the repulsion probabilities. Since the low average energy is obtained for similar conditions that minimize the maximum repulsion energy we can say that by satisfying conditions that

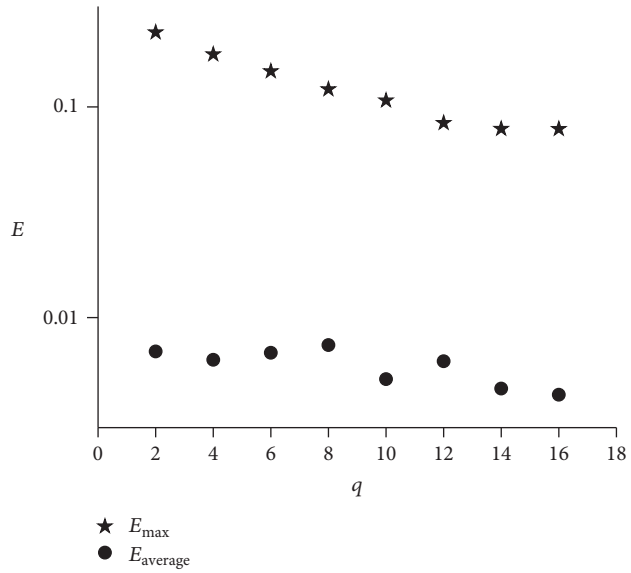

Figure 5: Bottom: average repulsive energy per wire in the bar code as function of the number of bars q (or narrowness of the bars); top: maximum repulsive energy for any wire in the configuration with q bars (located at the star position in previous figure).

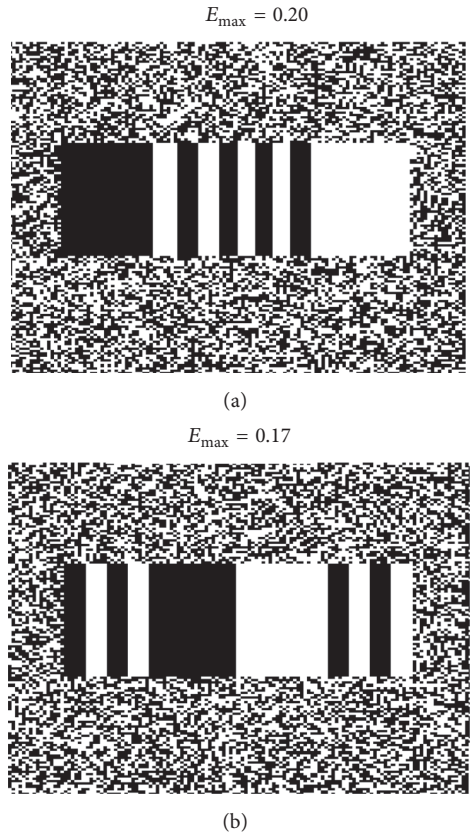

Figure 6: Scheme of two configurations mixing wide and narrow bands; the corresponding maximum repulsive energies are given on the top. To (a) wider bands are at the ends producing higher repulsive energy; to (b) wider bands are at the center slightly lowering the repulsive energy.

minimize the triggering of the reversal mechanism in the bar code we also minimize the propagation probability of any initiated reversal. This makes the information stored in these bar codes very reliable.

Our results are valid for long rods. As the length $2L$ of the wires increases we can observe from (1) through (2) that the most important effect of this variation is a decrease of all energies by a similar factor, which does not alter the relative energies leading to stabilization mechanisms. On the other hand, as the lattice constant d decreases the interaction energy between nearby wires ($D \approx d$) is greatly enlarged; this is even more so for wide wires ($b \to d/2$). These cases may lead to nonobvious changes for the results near the limits of the alternating bars. From the point of view of predictability it would be better to stay off dense lattices with fat wires.

Previous calculations ignore temperature since any possible applications of these systems would be intended to work at room temperature which means an excitation energy of approximately 0.025 eV. This is too small compared to the energy necessary for a magnetization reversal in these nanotubes, which is controlled by the material and geometry through the coercivity. For all practical cases reversal energies are of the order of a few hundred eV or higher, which makes the temperature effect negligible.

4. Conclusions

It is possible to minimize the magnetostatic repulsive energy among the nanowires defining magnetic bar codes storing coded information. Several features are at disposal in order to achieve this goal intended to prolong the useful life of the stored information.

Magnetostatic repulsive energy is minimized for sectors of similar total content pointing in each direction, namely, half of the magnetic nanowires with up magnetization and the other half with down magnetization, where up and down magnetization are perpendicular to the cross section defining the bar code itself (see Figure 1).

Previous result can be optimized by narrowing the widths of the bars or what is equivalent upon dividing the rectangular sector defining the code in a large number of bars. This effect is notorious for the first few divisions of the rectangular sector into bars; however, it soon tends to saturate so it is not necessary to use more bars than those strictly needed.

Since wide bars are necessary to produce a variety of information stored wider bars should be preferred towards the center of the coded area. By the same token, wide bars should be avoided at the ends of the code.

It is remarkable that previously desired characteristics of these magnetic code bars, namely, half of the magnetic moments in each direction, many narrow bars, and slightly wider bars located towards the center, make these codes not only more stable from the point of view of the magnetostatic energy but also more difficult to be found, read, and interpreted when "printed" on a document or package. Actually the external signal of the whole set is quite small and difficult

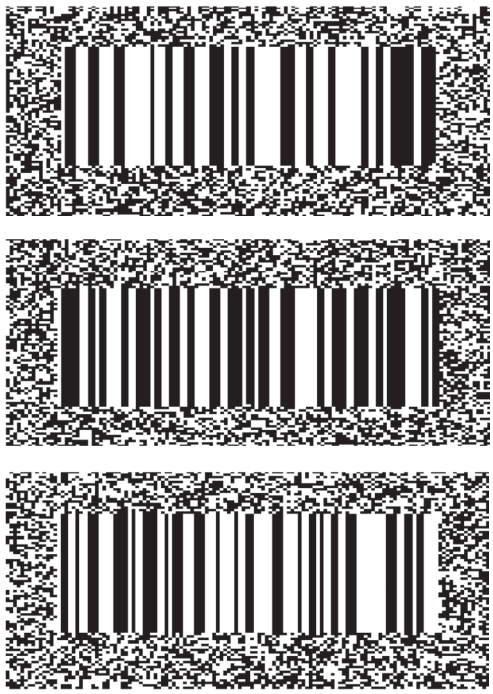

Figure 7: Portions of three bar codes for three different commercial products picked at random. The corresponding maximum energy is given to the right of the scheme presenting the magnetic bar code.

to read except for a magnetic tip position at the precise point and running in the right direction.

Disclosure

The present address of Julián Faúndez is Instituto de Física, Universidade Federal de Mato Grosso (UFMT), Cuiabá, Brazil.

Conflicts of Interest

The authors declare that there are no conflicts of interest regarding the publication of this paper.

Acknowledgments

This work was partially supported by Universidad de La Frontera under Projects DI16-2004 and DI17-0027. Partial support from the following Chilean sources is acknowledged: Fondecyt (Chile) under Contract 1150019 and Financiamiento Basal para Centros Cientficos y Tecnológicos de Excelencia (Chile) through the Center for Development of Nanoscience and Nanotechnology (CEDENNA, Contract FB0807).

References

[1] K. Nielsch, F. J. Castaño, S. Matthias, W. Lee, and C. A. Ross, "Synthesis of cobalt/polymer multilayer nanotubes," *Advanced Engineering Materials*, vol. 7, no. 4, pp. 217–221, 2005.

[2] V. D. R. Caffarena, J. L. Capitaneo, R. A. Simão, and A. P. Guimarães, "Preparation of electrodeposited cobalt nanowires," *Materials Research*, vol. 9, no. 2, pp. 205–208, 2006.

[3] J. Escrig, J. Bachmann, J. Jing, M. Daub, D. Altbir, and K. Nielsch, "Crossover between two different magnetization reversal modes in arrays of iron oxide nanotubes," *Physical Review B*, vol. 77, no. 21, Article ID 214421, 2008.

[4] E. E. Vogel, P. Vargas, S. Altbir, and J. Escrig, *Handbook of Nanophysics*, vol. 4, CRC Press, 2010, Edited by K. D. Sattler.

[5] M. S. Salem, P. Sergelius, R. M. Corona, J. Escrig, D. Görlitz, and K. Nielsch, "Magnetic properties of cylindrical diameter modulated $Ni_{80}Fe_{20}$ nanowires: interaction and coercive fields," *Nanoscale*, vol. 5, no. 9, pp. 3941–3947, 2013.

[6] Z. Haji Jamali, M. Almasi Kashi, A. Ramazani, and A. H. Montazer, "Unraveling the roles of thermal annealing and off-time duration in magnetic properties of pulsed electrodeposited NiCu nanowire arrays," *Journal of Applied Physics*, vol. 117, no. 17, Article ID 173905, 2015.

[7] M. Jaafar, J. Gómez-Herrero, A. Gil, P. Ares, M. Vázquez, and A. Asenjo, "Variable-field magnetic force microscopy," *Ultramicroscopy*, vol. 109, no. 6, pp. 693–699, 2009.

[8] E. Cisternas and E. E. Vogel, "Inscription and stabilization of ferromagnetic patterns on arrays of magnetic nanocylinders," *Journal of Magnetism and Magnetic Materials*, vol. 337-338, pp. 74–78, 2013.

[9] P. Landeros, S. Allende, J. Escrig, E. Salcedo, D. Altbir, and E. E. Vogel, "Reversal modes in magnetic nanotubes," *Applied Physics Letters*, vol. 90, no. 10, Article ID 102501, 2007.

[10] M. P. Proenca, C. T. Sousa, J. Escrig, J. Ventura, M. Vazquez, and J. P. Araujo, "Magnetic interactions and reversal mechanisms in Co nanowire and nanotube arrays," *Journal of Applied Physics*, vol. 113, no. 9, Article ID 093907, 2013.

[11] R. Skomski, E. Schubert, A. Enders, and D. J. Sellmyer, "Kondorski reversal in magnetic nanowires," *Journal of Applied Physics*, vol. 115, no. 17, Article ID 17D137, 2014.

[12] E. Cisternas and E. E. Vogel, "Improving information storage by means of segmented magnetic nanowires," *Journal of Magnetism and Magnetic Materials*, vol. 388, pp. 35–39, 2015.

[13] E. Cisternas, J. Faúndez, and E. E. Vogel, "Stabilization mechanisms for information stored in magnetic nanowire arrays," *Journal of Magnetism and Magnetic Materials*, vol. 426, pp. 588–593, 2017.

[14] C. Bran, E. Berganza, E. M. Palmero et al., "Spin configuration of cylindrical bamboo-like magnetic nanowires," *Journal of Materials Chemistry C*, vol. 4, no. 5, pp. 978–984, 2016.

[15] J. Yuan, W. Pei, T. Hasegawa et al., "Study on magnetization reversal of cobalt nanowire arrays by magnetic force microscopy," *Journal of Magnetism and Magnetic Materials*, vol. 320, no. 5, pp. 736–741, 2008.

[16] H. Zeng, M. Zheng, R. Skomski et al., "Magnetic properties of self-assembled Co nanowires of varying length and diameter," *Journal of Applied Physics*, vol. 87, no. 9, pp. 4718–4720, 2000.

[17] J. Escrig, S. Allende, D. Altbir, and M. Bahiana, "Magnetostatic interactions between magnetic nanotubes," *Applied Physics Letters*, vol. 93, no. 2, Article ID 023101, 2008.

[18] M. Beleggia, S. Tandon, Y. Zhu, and M. De Graef, "On the magnetostatic interactions between nanoparticles of arbitrary shape," *Journal of Magnetism and Magnetic Materials*, vol. 278, no. 1-2, pp. 270–284, 2004.

[19] E. Cisternas, Y. Vásquez, and E. E. Vogel, "Force among magnetic nanocylinders trapped in triangular arrays," *Journal of Magnetism and Magnetic Materials*, vol. 324, no. 6, pp. 1021–1029, 2012.